Chemistry Europe
European Chemical Societies Publishing

WILEY VCH

Excellence in Chemistry Research

Announcing our new flagship journal

- Gold Open Access
- Publishing charges waived
- Preprints welcome
- Edited by active scientists

Meet the Editors of *ChemistryEurope*

Luisa De Cola
Università degli Studi di Milano Statale, Italy

Ive Hermans
University of Wisconsin-Madison, USA

Ken Tanaka
Tokyo Institute of Technology, Japan

Chemistry–A European Journal
Research Article
doi.org/10.1002/chem.202300087
Chemistry Europe
European Chemical Societies Publishing
www.chemeurj.org

VIP Synthesis and Crystallographic Characterization of Helical Hairpin Oligourea Foldamers

Nagendar Pendem,[a, d] Yella-Reddy Nelli+,[a] Léonie Cussol,[a] Claude Didierjean,[b] Brice Kauffmann,[c] Christel Dolain,*[a] and Gilles Guichard*[a]

Abstract: Oligomers designed to form a helix-turn-helix super-secondary structure have been prepared by covalently bridging aliphatic oligourea foldamer helices with either rigid aromatic or more flexible aliphatic spacers. The relative helix orientation in these dimers was investigated at high resolution using X-ray diffraction analysis. In several cases, racemic crystallography was used to facilitate crystallization and structure determination. All structures were solved by direct methods. Well-defined parallel helical hairpin motifs were observed in all cases when 4,4′-methylene diphenyl diisocyanate was employed as a dimerizing agent, irrespective of primary sequence and chain length.

Introduction

Research within the field of foldamer chemistry has led to the design and discovery of a wide range of unnatural synthetic oligomers predisposed to adopt well-defined secondary structures akin to those found in biopolymers.[1] These encompass aliphatic peptidomimetic backbones (e.g., peptoids, β-peptides,[1a,2] γ-peptides,[2–3] sulfono-γ-AApeptides,[4] oligoureas[5]), backbones with no apparent similarity to natural systems (e.g., aromatic oligoamides[6]) and mixed α-peptide-foldamer backbones.[4,7] The structural knowledge of isolated secondary structures gained from these early studies paved the ground for research efforts aimed at creating more sophisticated architectures more closely approaching biopolymers in size and shape (and ideally function).[1c,8] In particular, substantial progress has been made in this direction with the characterization of extended and compact quaternary structures from foldamers designed to self-assemble.[9] Concurrently, connecting multiple individual folded segments may lead to unique tertiary structures, despite specific difficulties resulting from the need to design complementary surfaces between individual folded modules and the synthesis challenge to prepare long oligomeric strands.[10]

The helix-turn-helix (HTH) is a tertiary helical motif of intermediate complexity and a useful starting point to elaborate more sophisticated tertiary and self-assembled quaternary structures.[10g,11] In proteins, this motif – also named helical hairpin or helix-loop-helix – is highly prevalent and is formed by two antiparallel helices (α- and/or 3_{10}-) connected by a short turn/loop unit (typically 2–9 amino acid residues). Principles that govern helical hairpin formation in proteins have been studied extensively and successfully applied to de novo design.[12] X-ray structures of HTH peptides designed de novo from synthetic α-helices and appropriate interhelical turns generally demonstrate good agreement with design.[13] Natural and engineered helical hairpins have been used extensively as molecular scaffolds for applications ranging from inhibition of protein–protein interactions,[14] to enzyme mimicry[15] and the construction of peptide-based nanomaterials (e.g., synthetic helical nanotubes[11]).

Extensions to unnatural synthetic helical hairpins include the antiparallel (Gly_4 linker) and parallel (cystine linker) connection of 3_{10}-helices (nucleated with α-aminoisobutyric acid (Aib) or α,β-dehydrophenylalanine residues) whose structures were determined by X-ray diffraction (XRD).[16] Only a few foldamer-based HTH tertiary structures have been reported. These include parallel or antiparallel β-peptide or α,β-peptide helix dimers connected with various interhelical segments (e.g., D-Pro-Gly, cysteine, βGly_4 or longer peptides) and whose structures have been characterized in solution or by XRD.[14c,17] Helical aromatic oligoamides and rigid interhelical connectors have also been employed.[10e,g,18]

In this work, we set out to create helix-turn-helix (HTH) tertiary motifs from aliphatic oligoureas, a class of peptidomi-

[a] Dr. N. Pendem, Dr. Y.-R. Nelli,+ Dr. L. Cussol, Dr. C. Dolain, Dr. G. Guichard
Univ. Bordeaux, CNRS, Bordeaux INP, CBMN, UMR 5248
Institut Européen de Chimie et Biologie
33600 Pessac (France)
E-mail: c.dolain@iecb.u-bordeaux.fr
g.guichard@iecb.u-bordeaux.fr
[b] Dr. C. Didierjean
Université de Lorraine, CNRS, CRM2
54000 Nancy (France)
[c] Dr. B. Kauffmann
Univ. Bordeaux, CNRS, INSERM, IECB, UAR 3033
33600 Pessac (France)
[d] Dr. N. Pendem
Department of Chemistry
University of Washington
Seattle, Washington, 98195 (USA)
[+] Deceased: September 26, 2016

Supporting information for this article is available on the WWW under https://doi.org/10.1002/chem.202300087

metic helical foldamers, by using diamine-type connectors to bridge two helices head-to-head (Figure 1). Enantiopure urea homo-oligomers form well-defined H-bonded 2.5-helices[19] and structures for such oligomers ranging from five to 20 residues have been characterized at high resolution by X-ray diffraction.[9f,20] This robust and modular helical fold is thus well suited for the elaboration of new architectures involving multiple helices such as the HTH motif. We have evaluated two types of connectors, either short or rigid to orient helices at an angle or more flexible to allow helices to sample a broader region of space. We report crystallization efforts including racemic crystallization to gain structural insight into the relative arrangement of individual helices within the HTH motif.

Results and Discussion

Synthesis

The general synthesis approach to generate parallel HTH type motifs by dimerization of oligourea helices is outlined in Figure 1. The target molecules were constructed in a single step by reacting one equivalent of a bis-isocyanate linker with two equivalents of a urea oligomer bearing a free amino terminus (as trifluoroacetate salt) in dimethylformamide (DMF) using diisopropylethylamine (DIPEA) as base. We initially focused our study on three different all-hydrocarbon spacers: tetramethylene diisocyanate (TtMDI) and hexamethylene diisocyanate (HMDI) as flexible aliphatic spacers, and 4,4′-methylene-diphenyl diisocyanate (4,4′-MDI) as a rigid aromatic spacer. Different types of oligourea helices with proteinogenic aliphatic and aromatic side chains (R = Me, *i*Pr, *i*Bu, Bn) were selected – that is, two short hexaurea sequences $(Val^{u}Ala^{u}Leu^{u})_2$ (**1**, **2**, *ent*-**2**, **3** and *ent*-**3**) or $(Phe^{u})_6$ (**4** and *ent*-**4**) and a longer octaurea sequence $(Phe^{u})_8$ (**5** and *ent*-**5**) – to investigate the influence of the primary sequence and chain length on the formation of the HTH motif (Scheme 1). We prepared each target molecule by dimerization of the corresponding helical sequence with the corresponding linker in moderate to high yields (37–96%).

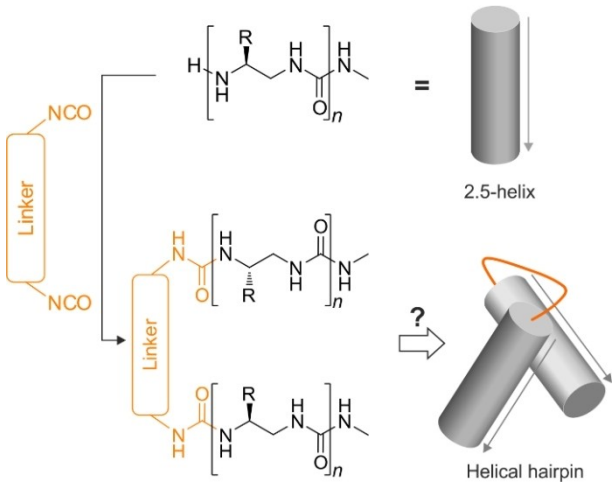

Figure 1. Proposed strategy to form covalently bridged head-to-head oligourea helices (helix-linker-helix, HTH motif) by reaction of a bis-isocyanate linker with amino-terminated urea oligomers.

Crystallization experiments and structure determination

Enantiopure compounds **1**, *ent*-**2** and *ent*-**3** derived from aliphatic sequences were crystallized from a DMSO solution and were characterized in the solid state by single-crystal XRD. However, in the case of aromatic sequences, all our efforts to either grow single crystals using various solvent conditions or to solve the structures (by direct methods or molecular replacement) of enantiopure compounds **4** and **5** remained unsuccessful. To overcome this difficulty, we decided to explore the use of racemic crystallization. The formation of single crystals suitable for XRD may be facilitated, and the problem of phase determination alleviated by crystallizing racemates.[7b,21] With

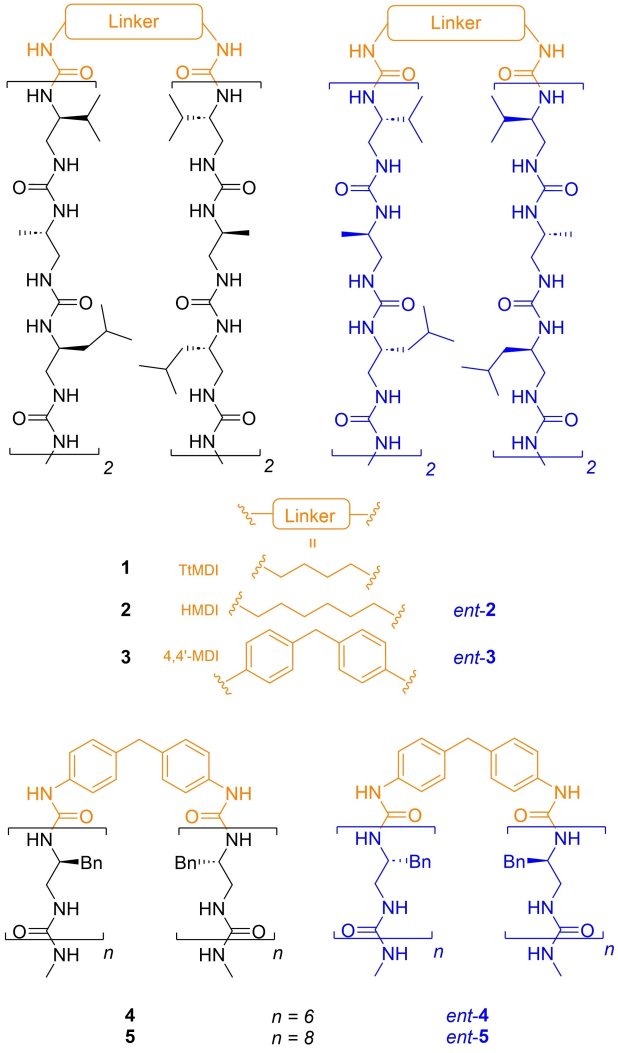

Scheme 1. Chemical structures of the different target compounds showing the nature of the linker, the corresponding enantiomer, the sequence and its length. Linker units are represented in orange, and enantiomers are represented in black or blue depending on their stereochemistry.

Table 1. X-ray data collection and refinement statistics.

	1	*ent*-**2**	*rac*-**2**	*ent*-**3**	*rac*-**4**	*rac*-**5**
Deposition no.	2013429	2013427	1973370	2013479	966606	966605
Formula	$C_{76}H_{154}N_{28}O_{14}$	$C_{78}H_{158}N_{28}O_{14}$	$C_{78}H_{158}N_{28}O_{14}$	$C_{85}H_{156}N_{28}O_{14}$	$C_{137}H_{164}N_{28}O_{14}$	$C_{177}H_{212}N_{36}O_{18}$
M [g mol^{-1}]	1683.20	1711.40	1711.40	1793.20	2425.30	3129.70
Solvent	DMSO	DMSO	DMF/MeOH	DMSO/$CHCl_3$/MeOH	DMF	DMF
Crystal system	orthorhombic	triclinic	monoclinic	orthorhombic	monoclinic	triclinic
Space group	$P2_12_12_1$	$P1$	$P2_1/c$	$P2_12_12_1$	$P2_1/n$	$P\bar{1}$
Unit-cell parameters [Å, °]	$a=13.85$	$a=10.88$	$a=19.32$	$a=11.43$	$a=13.08$	$a=19.94$
	$b=25.56$	$b=14.13$	$b=54.93$	$b=30.52$	$b=30.62$	$b=22.06$
	$c=27.33$	$c=17.90$	$c=19.65$	$c=33.61$	$c=35.70$	$c=22.74$
	$\alpha=90$	$\alpha=102.90$	$\alpha=90$	$\alpha=90$	$\alpha=90$	$\alpha=92.96$
	$\beta=90$	$\beta=97.52$	$\beta=91.64$	$\beta=90$	$\beta=94.81$	$\beta=94.13$
	$\gamma=90$	$\gamma=90.29$	$\gamma=90$	$\gamma=90$	$\gamma=90$	$\gamma=93.47$
Volume [Å^3]	9674	2658	20848	11726	14249	9943
Z	8	1	4	4	4	2
T [K]	130	130	100	130	100	100
ρ [g cm^{-3}]	1.157	1.167	1.121	1.157	1.122	1.126
λ [Å]	1.54178	1.54178	0.8103	1.54178	1.54178	0.873
No. of measured reflections	47718	19813	166066	115252	29640	191186
No. of unique reflections	12140	10974	26932	19594	10477	26098
Parameters/restraints	1085/0	1180/35	2284/122	1282/21	1308/63	2289/150
Goodness of fit	1.023	1.080	1.054	0.853	1.441	1.032
R_1	0.0795	0.0760	0.1159	0.0863	0.1627	0.0869
wR_2	0.1870	0.2215	0.3009	0.2528	0.4004	0.2376

the advent of protein chemical synthesis, racemic (and quasi-racemic) crystallization has been applied more systematically to solve structures of peptides and proteins reluctant to crystallize.[22] Similarly, crystallizing racemates or quasi-racemates has been found to be helpful in foldamer chemistry in difficult cases.[7b,23]

The enantiomers of compounds **2**–**5** were synthesized starting from monomer units of opposite configuration. Both enantiomers were prepared and then mixed in equal amount to produce the corresponding racemates which were subjected to co-crystallization experiments. Single crystals of *rac*-**2**, *rac*-**4** and *rac*-**5** were readily and rapidly obtained from a DMF solution and the structures of the three racemates were solved in centrosymmetric space groups by direct methods using SHELXD.[24] Data collection and refinement statistics for all six structures are shown in Table 1. In order to precisely describe and compare each of the six HTH crystal structures, three quantitative parameters were measured systematically: i) interhelical dihedral angle Ω, that is, degree of rotation between planes of two helices defined by axis vectors and perpendicular vector of closest approach,[2] ii) interhelical distance d, that is, distance between centroids, defined as the geometric center of all C^{β} atoms of each individual helix, iii) helical twist ω, that is, degree of rotation between helices defined by the orientation of the C^{β}–C^{γ} vectors of the first side chain of each individual helix (Figure S17 and Table S4 in the Supporting Information).

Modulation of the linker

To study the effect of the linker on the relative helix-helix orientation, we prepared enantiopure compounds **1**, *ent*-**2** and *ent*-**3** derived from aliphatic sequences. X-ray structure analysis reveals that compound **1** with the short TtMDI linker adopts an "open" conformation with the two right-handed oligourea helices arranging in an antiparallel orientation (Figure 2a).

The axes of the two helices connected by the tetramethylene spacer define an interhelical dihedral angle Ω of ~140° (Figure 2a, b) and are separated by a distance of ~11 Å. Assuming that the diameter of the 2.5 oligourea helix (without taking the side chains into account) is ~5.4–5.6 Å,[25] the TtMDI linker is too short to allow the helices to adopt a helical hairpin conformation. The observed "open" conformation might origi-

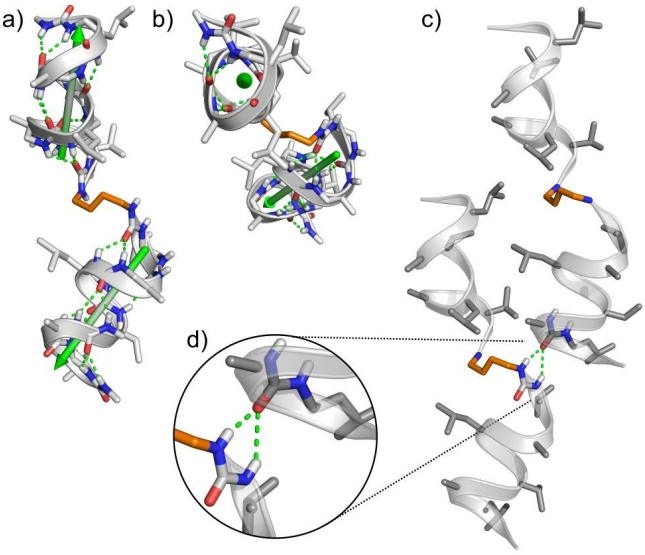

Figure 2. X-ray structure of **1**. a) Side and b) top views showing the open conformation with the TtMDI linker in orange. The helical axis of each helical segment is represented with vectors, showing an interhelical dihedral angle of ~140°. c) Crystal packing in a $P2_12_12_1$ unit cell showing hydrophobic effect and d) hydrogen bonding contacts between two molecules.

nate from packing arrangements in the crystal, through the hydrophobic effect and a three-centered hydrogen bond between two urea NHs close to the linker on one molecule and the terminal CO of the second molecule (Figure 2c, d). The two helical segments are well-conserved and superimpose well as indicated by the root mean square deviation (RMSD) of 0.256 Å calculated by fitting the six pairs of β-carbons (i.e., CH(R) in the monomer units). Based on this first result, we decided to extend the length of the linker by two methylene units, extending the tetramethylene to a hexamethylene spacer, to allow the two helical segments to adopt a hairpin conformation. The X-ray structures of homochiral compound *ent*-**2** and of the corresponding racemate *rac*-**2** were solved in the chiral space group *P*1 and the achiral centrosymmetric space group $P2_1/c$ (two independent molecules in the asymmetric unit), respectively.

It is noteworthy that both structures show the presence of a helical hairpin, confirming our previous hypothesis. The axes of the two helices in the hairpin run almost parallel in all the structures (one hairpin in *ent*-**2** and the two independent molecules in *rac*-**2**; Figure 3a, d). Despite the similar relative orientation of the connected helices in all three structures, the hexamethylene connector was found to span three different conformations, resulting in small variations in the interhelical dihedral angle Ω (4.1 to 32.6 °) and in the distance between the two connecting nitrogen atoms of the spacer (d(N,N) ranging from ~7.3–7.8 Å) (Figure 3e, f). In these three structures, the two helices forming the hairpin are rotated approximately 150–170° (ω) relative to each other along their axis. The outcome is that the two isobutyl side chain of Leu^{u}3 face each other within a short distance (4.6–5.7 Å between the $^{\delta}$C of the two side chains) thus contributing to the formation of a hydrophobic core in the hairpin. The structure of *ent*-**3** reveals that the more rigid 4,4′-MDI linker also preserves the parallel orientation of the two helices in the hairpin but the geometry of the linker imposes a different relative orientation of the two helices which in this case are rotated by 120–130° (ω) along their axis (Figure 4a, b). The interhelical distance of about 12 Å is similar compared to that measured with the HMDI linker. The structure shows two pairs of side chains facing each other within a relatively short distance in the center of the hairpin. The distance between the $^{\delta}$C of the two Leu^{u}3 is 5.6 Å and that between the methyl groups of Ala^{u}5 residues is 5.1 Å. In both the crystals of *ent*-**2** and *ent*-**3**, the hairpins are packed head-to-tail vertically in a complementary H-bond network involving the terminal urea NHs of one hairpin and terminal carbonyl groups on another hairpin (Figure 4c, d). This head-to-tail arrangement is reminiscent of the most common packing mode of individual helices observed in previously reported X-ray structures of oligoureas.[20a]

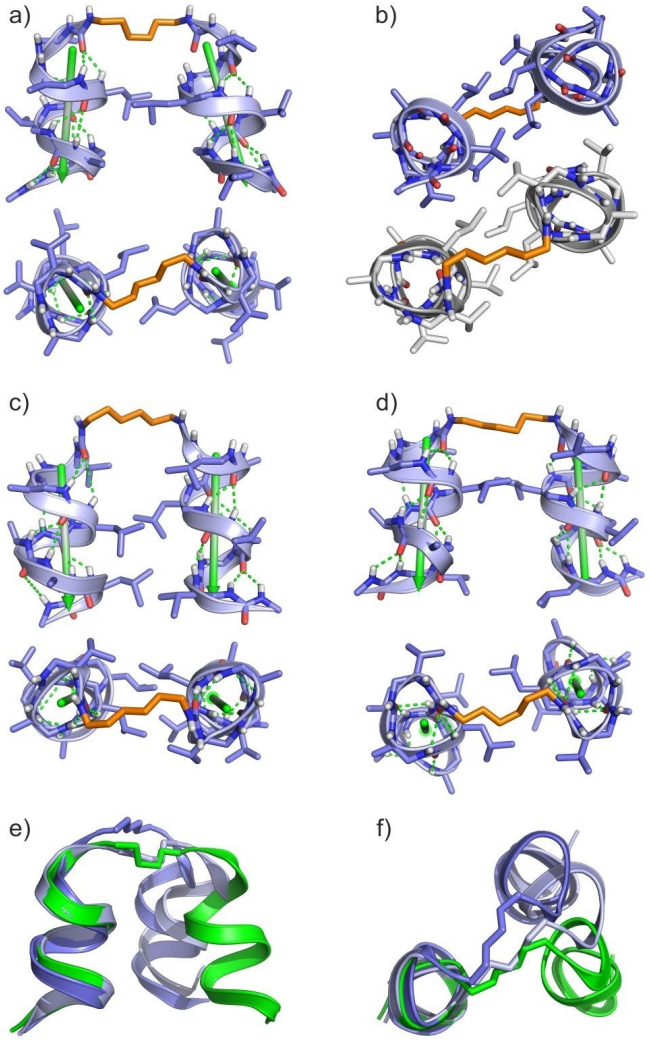

Figure 3. a) X-ray structure of *ent*-**2**, side and top views showing the hairpin conformation with the HMDI linker in orange. b) X-ray structure of *rac*-**2**, showing **2** and *ent*-**2**. c), d) X-ray structures of the two independent left-handed molecules in *rac*-**2** showing the two different conformations of the linker. e), f) Superimposition along the first helical segment (fitting of the six β-carbons) of the three conformations (*ent*-**2** in green and *rac*-**2** in gray and light blue), showing angle variations and different orientations of the second helical segment.

Modulation of the sequence and chain length

The influence of the primary sequence on the formation and the geometry of the resulting HTH motif was further investigated using the 4,4′-MDI linker. The X-ray structure of *rac*-**4** which contains only Phe^{u} residues shows a helical hairpin with the two right-handed oligourea helices parallel to the hairpin axis similar to the conformation observed for *ent*-**3** (Figure 5). The two helical segments in the hairpin superimpose well as indicated by the root mean square deviation (RMSD) of 0.382 Å calculated by fitting the six pairs of β-carbons. The axes of the two helices connected by the 4,4′-methylene-diphenyl spacer are separated by a distance of ~12.1 Å. The internal space defined by two helices is thus sufficient for benzyl side chains of each segment to interact intramolecularly by aromatic π-stacking within the hairpin. These interactions are best illustrated by the aromatic ring of Phe^{u}3 in one of the helices which is involved in multiple contacts with edge-to-face and parallel-displaced geometries with corresponding Phe^{u}2, Phe^{u}3 and Phe^{u}5 residues of the neighboring helix (Figure 5b).[26] In the crystal, the two enantiomers are packed along the edge of

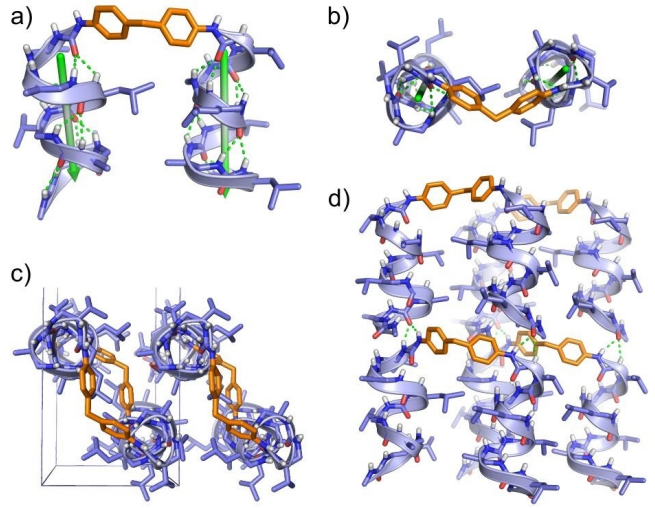

Figure 4. X-ray structure of *ent*-**3**. a) Side and b) top views showing the hairpin conformation with the 4,4′-MDI linker in orange. c), d) Crystal packing in a chiral $P2_12_12_1$ unit cell, showing the vertical head-to-tail arrangement through intermolecular hydrogen bonds between the terminal urea NHs of one hairpin and terminal carbonyl groups on another hairpin.

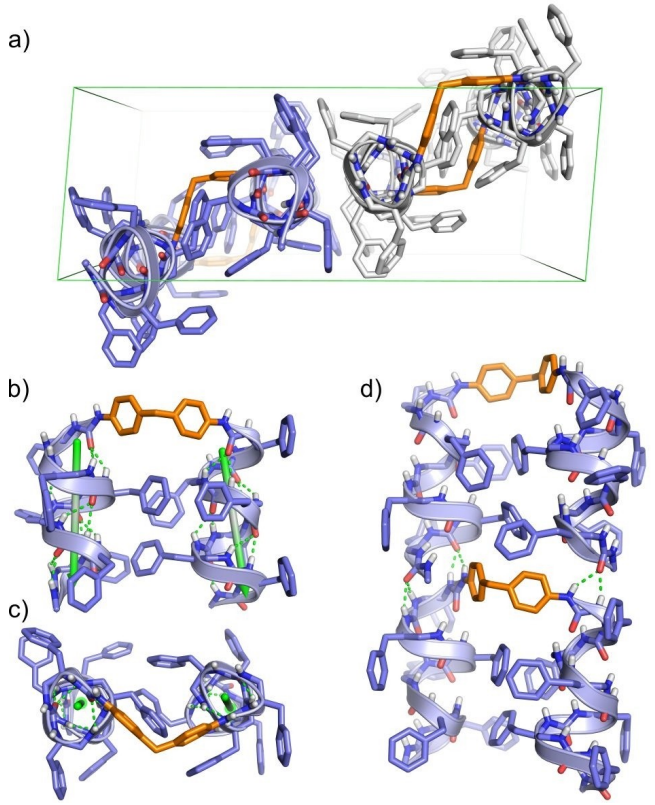

Figure 5. X-ray structure of *rac*-**4**. a) Racemic crystal packing in a centrosymmetric $P2_1/n$ unit cell showing **4** (gray) and *ent*-**4** (light blue) with the 4,4′-MDI linker in orange. b) Structure of the hairpin structure in *ent*-**4** viewed parallel to the hairpin axis and c) top view, showing interactions between benzyl side chains. d) Vertical head-to-tail arrangement through intermolecular hydrogen bonds between six terminal urea NHs of one hairpin and three terminal carbonyl groups on another hairpin.

the hairpin to create a centrosymmetric interface. Again a vertical head-to-tail packing is observed (Figure 5d) involving extensive hydrogen bonding contacts, that is, six intermolecular H-bonds formed at each end (involving four terminal NHs on one helix of the hairpin and two NHs on the second).

To evaluate whether a similar hairpin type structure also forms when longer helical segments are connected by 4,4′-MDI, we prepared cognate oligomer **5** (Phe^u_8). Two different sets of crystals of enantiopure **5** were obtained in parallel. For the first set of crystals, diffraction data were collected at different wavelengths (on a home source at the Mo and $Cu_{K\alpha}$ wavelengths and at a synchrotron (ID29)). In all cases, the data were indexed in the space group $P2_12_12_1$ with similar unit cell parameters. However, all attempts to solve the structure by direct methods using SHELXD and SHELXT and by molecular replacement have been unsuccessful. This might be related to the presence of many symmetry-independent molecules in the asymmetric unit cell ($Z=8$) and the relative small size of the search model.

Compounds **5** and *ent*-**5** were obtained from 4,4′-MDI and the corresponding octaurea in 77 and 88% yield, respectively. We were able to grow single crystals of *rac*-**5** in pure DMF, the structure was readily solved by direct methods. Oligomer *rac*-**5** crystallized in the achiral centrosymmetric space group $P\bar{1}$ with one molecule of each **5** and *ent*-**5** forming the unit cell. The arrangement of enantiomeric molecules in the unit cells differs from that of *rac*-**4**. The two enantiomeric hairpins are organized in a face-to-face centrosymmetric arrangement with a large contact surface (calculated buried surface ~200 Å^2) involving multiple π-π interactions (Figure 6a). The helical hairpin structure of **5** is similar to that of **4**, featuring an almost perfect parallel orientation of the helices ($\Omega=0.6°$) and multiple intramolecular interhelical π-π interactions (Figure 6c, d). The mean backbone torsion angles of each helix are very close to that previously reported for a cognate helical octamer (CCDC no. 750017[20a]). Two well-defined DMF molecules are inserted in the free space between the two helices of the hairpin (Figure 6e). Homochiral helical hairpins are aligned end-to-end in a columnar arrangement, the four NHs of the ureas connected to MDI in one hairpin being H-bonded to the carbonyls of the first two residues of a second hairpin (Figure 6b).

Conclusions

The design of synthetic, sequence-specific, helically folded molecules has attracted considerable interest, in part because of their potential applications as α-helix or DNA mimics, as receptors for molecular guests, as catalysts or as self-assembling units to create quaternary structures. Functional sequences generally correspond to isolated helices, but more sophisticated motifs such as the HTH motif obtained by connecting two helical foldamers together to create a simple tertiary structure with two helices running (anti)parallel or oriented at an angle[10e,g,14c] are of interest to further expand the recognition potential of foldamers and improve their functions. As a first step towards the creation of urea-based foldamers that mimic

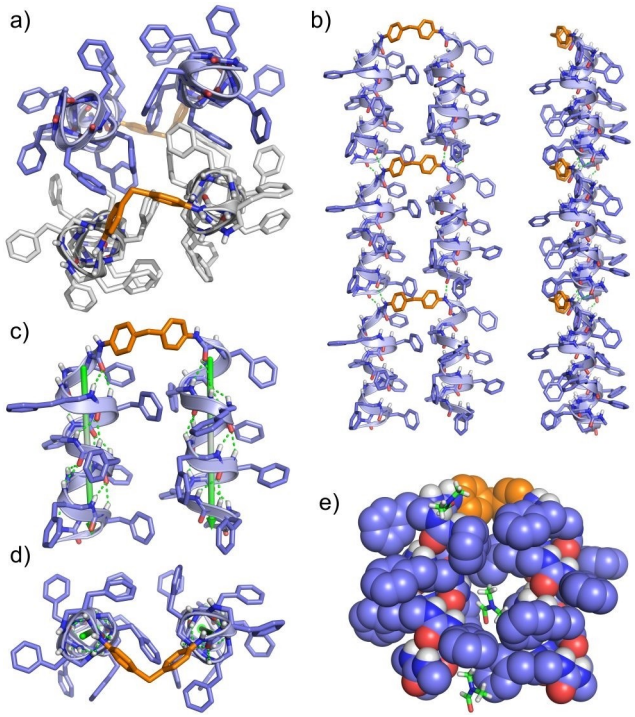

Figure 6. X-ray structure of *rac*-**5**. a) Racemic crystal packing in a centrosymmetric $P\bar{1}$ unit cell showing **5** (gray) and *ent*-**5** (light blue) with the 4,4′-MDI linker in orange. b) Vertical head-to-tail arrangement through intermolecular hydrogen bonds between four terminal urea NHs of one hairpin and two terminal carbonyl groups on another hairpin. c) Structure of the hairpin in *ent*-**5** viewed parallel to the hairpin axis and d) top view showing interactions between benzyl side chains. e) CPK representation showing the presence of solvent molecules in the free space.

protein HTH super-secondary motifs, we prepared a series of covalent dimers of oligourea helices by using bis-isocyanates as connectors and determined the resulting structures at atomic resolution. In two cases (oligomers **4** and **5**), racemic crystallization[7b,21] proved decisive in overcoming difficulties with crystal growth and phasing. The corresponding racemates *rac*-**4** and *rac*-**5** readily crystallized in centrosymmetric space groups, thus allowing the structures to be solved by direct methods. Various linkers were employed to modulate the overall conformation and explore interactions between helices. Helix hairpin structures were obtained when using either the flexible HMDI connector or the more rigid 4,4′-MDI linker. Both spacers appear to be well suited to hold the two helical segments with a parallel orientation of their axes, and at a distance that allows inter-helical contacts. It is noteworthy that, depending on the choice of the linker, it is possible to modulate the relative orientation of the two helices in the hairpin (i.e., helical twist ω, see Figure S17 for definition). Fine tuning the ω value may be particularly useful for optimizing intramolecular interactions and orienting specific side chains toward the solvent. Studies aimed at accelerating the preparation of such helical hairpin oligourea foldamers by using solid-phase synthesis and at designing water-soluble sequences for self-assembly or for recognizing extended proteins surfaces are underway in our laboratory and will be reported in due course.

Experimental Section

General procedure: Boc-protected hexaureas and octaurea were synthesized in solution using a stepwise approach and N-Boc protected succinimidyl carbamate building blocks following previously reported procedures.[20] Boc protected-oligourea (0.1 mmol) was treated with TFA (2 mL) at 0 °C for 30 min. After completion of the reaction, followed by TLC, the solvent was first evaporated under reduced pressure and then co-evaporated with cyclohexane. TFA salt was dissolved in DMF (2 mL) and cooled down to 0 °C. DIPEA (3 equiv., 0.3 mmol) was added followed by the addition of the corresponding diisocyanate (0.5 equiv., 0.05 mmol). The reaction mixture was stirred at room temperature overnight. After completion of the reaction, the solvent was evaporated and a saturated $NaHCO_3$ solution was added, a precipitate was formed which was filtered off and washed with various solvents (sat. $NaHCO_3$, 1 M $KHSO_4$, water, DCM, brine) and finally dried under high vacuum to yield the desired compound.

Synthesis of compound 3: Compound **3** was prepared following the general procedure in 91 % coupling yield. ^{1}H NMR (400 MHz, CD_3OH): $\delta = 8.23$ (s, 2H), 7.25 (d, $J = 8$ Hz, 4H), 7.07 (d, $J = 8$ Hz, 4H), 6.54–6.31 (m, 10H), 6.23–6.20 (m, 2H), 6.10–5.89 (m, 12H), 5.84 (d, $J = 9$ Hz, 2H), 4.11–3.98 (m, 2H), 3.97–3.74 (m, 10H), 3.72–3.49 (m, 14H), 2.70 (d, $J = 4$ Hz, 6H), 2.66–2.51 (m, 4H), 2.48–2.26 (m, 8H), 1.80–1.49 (m, 8H), 1.35–1.11 (m, 8H), 1.04–0.82 ppm (m, 60H). ^{13}C NMR (100 MHz, CD_3OH): $\delta = 162.1$, 162.0, 161.8, 161.8, 161.4, 160.9, 159.0, 138.8, 137.1, 130.2, 120.4, 56.1, 47.2, 46.9, 46.3, 46.1, 44.6, 43.8, 42.7, 41.2, 32.0, 31.9, 26.8, 26.2, 25.8, 23.6, 22.7, 22.4, 20.1, 20.0, 18.8, 18.4, 18.3 ppm. MALDI-TOF MS (M_W 1793.2): *m/z* 1794.4 $[M+H]^+$.

X-ray crystallography: Single crystals were obtained by slow evaporation method. Enantiopure compounds **1**, *ent*-**2** and *ent*-**3** crystallized from a DMSO solution. Single crystals of *rac*-**2**, *rac*-**4** and *rac*-**5** were readily and rapidly obtained from a DMF solution. Typically, the crystals were obtained in around 1 to 2 weeks and suitable single crystals were picked for X-ray diffraction analysis.

All crystal structures were solved using direct methods implemented in SHELXD[24] and were refined using SHELXL 2013[27] version. Full matrix least-squares refinement were performed on F2 for all unique reflections, minimizing $w(F_o^2-F_c^2)^2$, with anisotropic displacement parameters for non-hydrogen atoms. Hydrogen atoms were positioned in idealized positions and refined with a riding model, with Uiso constrained to 1.2 Ueq value of the parent atom (1.5 Ueq when CH_3). The positions and isotropic displacement parameters of the remaining hydrogen atoms were refined freely. SHELXL DFIX and RIGU commands were used to restrain some side chains as rigid groups and restrain their displacement parameters. The solvent flattening squeeze procedure implemented in Platon[28] was used to treat disorder in the solvent regions of the crystals for compound **1**, *rac*-**2**, *rac*-**4** and *rac*-**5**. Data statistics are presented in the Table 1.

Deposition Numbers 2013429 (for **1**), 2013427 (for *ent*-**2**), 1973370 (for *rac*-**2**), 2013479 (for *ent*-**3**), 966606 (for *rac*-**4**), 966605 (for *rac*-**5**) contain the supplementary crystallographic data for this paper. These data are provided free of charge by the joint Cambridge Crystallographic Data Centre and Fachinformationszentrum Karlsruhe Access Structures service.

Acknowledgements

This work was supported in part by the Centre National de la Recherche Scientifique (CNRS) and Univ. Bordeaux. C.D. re-

ceived support from the CNRS through the program Emergence@INC2020. A predoctoral fellowship to L.C. from the Ministère de l'Enseignement Supérieur de la Recherche et de l'Innovation (pre-doctoral fellowship to L.C.) is gratefully acknowledged. This work has benefited from the facilities and expertise of IECB Biophysical and Structural Chemistry platform (BPCS), CNRS UMS3033, Inserm US001, Univ. Bordeaux. The ESRF CRG BM30A FIP and ID29 staff is gratefully acknowledged for beamtime and support for data collection. We thank Dr Jean-Christophe Taveau for helpful discussions and Dr Gavin W. Collie for critical appraisal of this manuscript prior to submission.

Conflict of Interests

The authors declare no conflict of interest.

Data Availability Statement

The data that support the findings of this study are available in the supplementary material of this article.

Keywords: foldamers · helices · racemic crystallography · tertiary structures · X-ray diffraction

[1] a) S. H. Gellman, *Acc. Chem. Res.* **1998**, *31*, 173–180; b) G. Guichard, I. Huc, *Chem. Commun.* **2011**, *47*, 5933–5941; c) W. S. Horne, T. N. Grossmann, *Nat. Chem.* **2020**, *12*, 331–337.
[2] D. Seebach, A. K. Beck, D. J. Bierbaum, *Chem. Biodiv.* **2004**, *1*, 1111–1239.
[3] B. Legrand, L. T. Maillard, *ChemPlusChem* **2021**, *86*, 629–645.
[4] P. Sang, Y. Shi, B. Huang, S. Xue, T. Odom, J. Cai, *Acc. Chem. Res.* **2020**, *53*, 2425–2442.
[5] S. H. Yoo, B. Li, C. Dolain, M. Pasco, G. Guichard in *Methods in Enzymology, Vol. 656* (Ed.: E. J. Petersson), Academic Press, **2021**, pp. 59–92.
[6] a) I. Huc, *Eur. J. Org. Chem.* **2004**, 17–29; b) D.-W. Zhang, X. Zhao, J.-L. Hou, Z.-T. Li, *Chem. Rev.* **2012**, *112*, 5271–5316; c) Y. Ferrand, I. Huc, *Acc. Chem. Res.* **2018**, *51*, 970–977.
[7] a) W. S. Horne, S. H. Gellman, *Acc. Chem. Res.* **2008**, *41*, 1399–1408; b) M. Kudo, V. Maurizot, B. Kauffmann, A. Tanatani, I. Huc, *J. Am. Chem. Soc.* **2013**, *135*, 9628–9631; c) J. Fremaux, L. Mauran, K. Pulka-Ziach, B. Kauffmann, B. Odaert, G. Guichard, *Angew. Chem. Int. Ed.* **2015**, *54*, 9816–9820; *Angew. Chem.* **2015**, *127*, 9954–9958.
[8] Z. E. Reinert, W. S. Horne, *Org. Biomol. Chem.* **2014**, *12*, 8796–8802.
[9] a) D. S. Daniels, E. J. Petersson, J. X. Qiu, A. Schepartz, *J. Am. Chem. Soc.* **2007**, *129*, 1532–1533; b) W. S. Horne, J. L. Price, S. H. Gellman, *Proc. Natl. Acad. Sci. USA* **2008**, *105*, 9151–9156; c) M. W. Giuliano, W. S. Horne, S. H. Gellman, *J. Am. Chem. Soc.* **2009**, *131*, 9860–9861; d) M. P. Del Borgo, A. I. Mechler, D. Traore, C. Forsyth, J. A. Wilce, M. C. J. Wilce, M.-I. Aguilar, P. Perlmutter, *Angew. Chem. Int. Ed.* **2013**, *52*, 8266–8270; *Angew. Chem.* **2013**, *125*, 8424–8428; e) V. Pavone, S.-Q. Zhang, A. Merlino, A. Lombardi, Y. Wu, W. F. DeGrado, *Nat. Commun.* **2014**, *5*, 3581; f) G. W. Collie, K. Pulka-Ziach, C. M. Lombardo, J. Fremaux, F. Rosu, M. Decossas, L. Mauran, O. Lambert, V. Gabelica, C. D. Mackereth, G. Guichard, *Nat. Chem.* **2015**, *7*, 871–878; g) P. S. P. Wang, A. Schepartz, *Chem. Commun.* **2016**, *52*, 7420–7432; h) K. H. Chen, K. A. Corro, S. P. Le, J. S. Nowick, *J. Am. Chem. Soc.* **2017**, *139*, 8102–8105; i) S. H. Yoo, H.-S. Lee, *Acc. Chem. Res.* **2017**, *50*, 832–841; j) G. Collie, C. M. Lombardo, S. H. Yoo, K. Pulka-Ziach, V. Gabelica, C. D. Mackereth, F. Rosu, G. Guichard, *Chem. Commun.* **2021**, *57*, 9514–9517.
[10] a) N. Delsuc, F. Godde, B. Kauffmann, J. M. Leger, I. Huc, *J. Am. Chem. Soc.* **2007**, *129*, 11348–11349; b) J. E. Ross, P. C. Knipe, S. Thompson, A. D. Hamilton, *Chem. Eur. J.* **2015**, *21*, 13518–13521; c) K. L. George, W. S. Horne, *J. Am. Chem. Soc.* **2017**, *139*, 7931–7938; d) A. G. Kreutzer, S. Yoo, R. K. Spencer, J. S. Nowick, *J. Am. Chem. Soc.* **2017**, *139*, 966–975; e) S. De, B. Chi, T. Granier, T. Qi, V. Maurizot, I. Huc, *Nat. Chem.* **2018**, *10*, 51–57; f) C. M. Lombardo, V. Kumar, C. Douat, F. Rosu, J. L. Mergny, G. F. Salgado, G. Guichard, *J. Am. Chem. Soc.* **2019**, *141*, 2516–2525; g) D. Mazzier, S. De, B. Wicher, V. Maurizot, I. Huc, *Angew. Chem. Int. Ed.* **2020**, *59*, 1606–1610; *Angew. Chem.* **2020**, *132*, 1623–1627; h) J. Atcher, P. Mateus, B. Kauffmann, F. Rosu, V. Maurizot, I. Huc, *Angew. Chem. Int. Ed.* **2020**, *60*, 2574–2577; i) M. Bejger, P. Fortuna, M. Drewniak-Świtalska, J. Plewka, W. Rypniewski, Ł. Berlicki, *Chem. Commun.* **2021**, *57*, 6015–6018.
[11] S. A. Hughes, F. Wang, S. Wang, M. A. B. Kreutzberger, T. Osinski, A. Orlova, J. S. Wall, X. Zuo, E. H. Egelman, V. P. Conticello, *Proc. Natl. Acad. Sci. USA* **2019**, *116*, 14456–14464.
[12] D. E. Engel, W. F. DeGrado, *Proteins* **2005**, *61*, 325–337.
[13] S. J. Lahr, D. E. Engel, S. E. Stayrook, O. Maglio, B. North, S. Geremia, A. Lombardi, W. F. DeGrado, *J. Mol. Biol.* **2005**, *346*, 1441–1454.
[14] a) K. Enander, G. T. Dolphin, L. Baltzer, *J. Am. Chem. Soc.* **2004**, *126*, 4464–4465; b) A. M. Watkins, M. G. Wuo, P. S. Arora, *J. Am. Chem. Soc.* **2015**, *137*, 11622–11630; c) J. W. Checco, D. F. Kreitler, N. C. Thomas, D. G. Belair, N. J. Rettko, W. L. Murphy, K. T. Forest, S. H. Gellman, *Proc. Natl. Acad. Sci. USA* **2015**, *112*, 4552–4557; d) D. Fujiwara, H. Kitada, M. Oguri, T. Nishihara, M. Michigami, K. Shiraishi, E. Yuba, I. Nakase, H. Im, S. Cho, J. Y. Joung, S. Kodama, K. Kono, S. Ham, I. Fujii, *Angew. Chem. Int. Ed.* **2016**, *55*, 10612–10615; *Angew. Chem.* **2016**, *128*, 10770–10773; e) J. Sadek, M. G. Wuo, D. Rooklin, A. Hauenstein, S. H. Hong, A. Gautam, H. Wu, Y. Zhang, E. Cesarman, P. S. Arora, *Nat. Commun.* **2020**, *11*, 1786; f) H. Adihou, R. Gopalakrishnan, T. Förster, S. M. Guéret, R. Gasper, S. Geschwindner, C. Carrillo García, H. Karatas, A. V. Pobbati, M. Vazquez-Chantada, P. Davey, C. M. Wassvik, J. K. S. Pang, B. S. Soh, W. Hong, E. Chiarparin, D. Schade, A. T. Plowright, E. Valeur, M. Lemurell, T. N. Grossmann, H. Waldmann, *Nat. Commun.* **2020**, *11*, 5425; g) M. Hussain, M. C. Cummins, S. Endo-Streeter, J. Sondek, B. Kuhlman, *J. Biol. Chem.* **2021**, *297*, 101348.
[15] a) S. Olofsson, G. Johansson, L. Baltzer, *J. Chem. Soc. Perkin Trans. 2* **1995**, 2047–2056; b) P. Rossi, P. Tecilla, L. Baltzer, P. Scrimin, *Chem. Eur. J.* **2004**, *10*, 4163–4170; c) J. Razkin, H. Nilsson, L. Baltzer, *J. Am. Chem. Soc.* **2007**, *129*, 14752–14758.
[16] Rudresh, S. Ramakumar, U. A. Ramagopal, Y. Inai, S. Goel, D. Sahal, V. S. Chauhan, *Structure* **2004**, *12*, 389–396.
[17] a) R. P. Cheng, W. F. DeGrado, *J. Am. Chem. Soc.* **2002**, *124*, 11564–11565; b) G. V. Sharma, V. Subash, K. Narsimulu, A. R. Sankar, A. C. Kunwar, *Angew. Chem. Int. Ed.* **2006**, *45*, 8207–8210; *Angew. Chem.* **2006**, *118*, 8387–8390; c) E. J. Petersson, A. Schepartz, *J. Am. Chem. Soc.* **2008**, *130*, 821–823; d) M. Drewniak, E. Węglarz-Tomczak, K. Ożga, E. Rudzińska-Szostak, K. Macegoniuk, J. M. Tomczak, M. Bejger, W. Rypniewski, Ł. Berlicki, *Bioorg. Chem.* **2018**, *81*, 356–361.
[18] H.-Y. Hu, J.-F. Xiang, Y. Yang, C.-F. Chen, *Org. Lett.* **2007**, *10*, 69–72.
[19] a) V. Semetey, D. Rognan, C. Hemmerlin, R. Graff, J.-P. Briand, M. Marraud, G. Guichard, *Angew. Chem. Int. Ed.* **2002**, *41*, 1893–1895; *Angew. Chem.* **2002**, *114*, 1973–1975; b) L. Fischer, G. Guichard, *Org. Biomol. Chem.* **2010**, *8*, 3101–3117.
[20] a) L. Fischer, P. Claudon, N. Pendem, E. Miclet, C. Didierjean, E. Ennifar, G. Guichard, *Angew. Chem. Int. Ed.* **2010**, *49*, 1067–1070; *Angew. Chem.* **2010**, *122*, 1085–1088; b) J. Fremaux, L. Fischer, T. Arbogast, B. Kauffmann, G. Guichard, *Angew. Chem. Int. Ed.* **2011**, *50*, 11382–11385; *Angew. Chem.* **2011**, *123*, 11584–11587; c) N. Pendem, C. Douat, P. Claudon, M. Laguerre, S. Castano, B. Desbat, D. Cavagnat, E. Ennifar, B. Kauffmann, G. Guichard, *J. Am. Chem. Soc.* **2013**, *135*, 4884–4892.
[21] a) A. L. Mackay, *Nature* **1989**, *342*, 133–133; b) L. E. Zawadzke, J. M. Berg, *Proteins Struct. Funct. Bioinf.* **1993**, *16*, 301–305; c) M. Doi, M. Inoue, K. Tomoo, T. Ishida, Y. Ueda, M. Akagi, H. Urata, *J. Am. Chem. Soc.* **1993**, *115*, 10432–10433; d) J. M. Berg, L. E. Zawadzke, *Curr. Opin. Biotechnol.* **1994**, *5*, 343–345; e) C. Toniolo, C. Peggion, M. Crisma, F. Formaggio, X. Shui, D. S. Eggleston, *Nat. Struct. Mol. Biol.* **1994**, *1*, 908–914; f) S. W. Wukovitz, T. O. Yeates, *Nat. Struct. Mol. Biol.* **1995**, *2*, 1062–1067; g) W. R. Patterson, D. H. Anderson, W. F. Degrado, D. Cascio, D. Eisenberg, *Protein Sci.* **1999**, *8*, 1410–1422.
[22] a) T. O. Yeates, S. B. H. Kent, *Annu. Rev. Biophys.* **2012**, *41*, 41–61; b) B. W. Matthews, *Protein Sci.* **2009**, *18*, 1135–1138; c) B. L. Pentelute, Z. P. Gates, V. Tereshko, J. L. Dashnau, J. M. Vanderkooi, A. A. Kossiakoff, S. B. Kent, *J. Am. Chem. Soc.* **2008**, *130*, 9695–9701; d) M. Avital-Shmilovici, K. Mandal, Z. P. Gates, N. B. Phillips, M. A. Weiss, S. B. H. Kent, *J. Am. Chem. Soc.* **2013**, *135*, 3173–3185; e) K. Mandal, B. L. Pentelute, D. Bang, Z. P. Gates, V. Y. Torbeev, S. B. H. Kent, *Angew. Chem. Int. Ed.* **2012**, *51*, 1481–1486; *Angew. Chem.* **2012**, *124*, 1510–1515; f) D. E. Mortenson, K. A. Satyshur, I. A. Guzei, K. T. Forest, S. H. Gellman, *J. Am. Chem. Soc.* **2012**, *134*, 2473–2476.

[23] M. Lee, J. Shim, P. Kang, I. A. Guzei, S. H. Choi, *Angew. Chem. Int. Ed.* **2013**, *52*, 12564–12567; *Angew. Chem.* **2013**, *125*, 12796–12799.
[24] G. Sheldrick, *Acta Crystallogr. Sect. A* **2008**, *64*, 112–122.
[25] Y. R. Nelli, L. Fischer, G. W. Collie, B. Kauffmann, G. Guichard, *Biopolymers* **2013**, *100*, 687–697.
[26] E. A. Meyer, R. K. Castellano, F. Diederich, *Angew. Chem. Int. Ed.* **2003**, *42*, 1210–1250; *Angew. Chem.* **2003**, *115*, 1244–1287.
[27] G. Sheldrick, *Acta Crystallogr. Sect. C* **2015**, *71*, 3–8.
[28] A. L. Spek, *Acta Crystallogr. Sect. C* **2015**, *71*, 9–19.

Manuscript received: January 12, 2023
Accepted manuscript online: March 21, 2023
Version of record online: ■■, ■■

RESEARCH ARTICLE

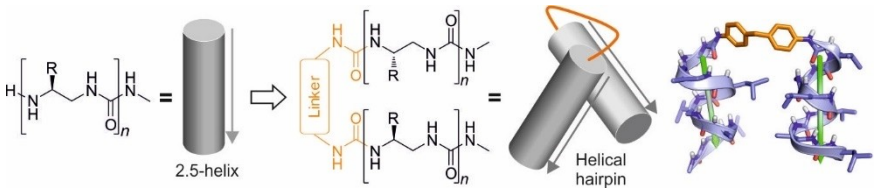

Dr. N. Pendem, Dr. Y.-R. Nelli, Dr. L. Cussol, Dr. C. Didierjean, Dr. B. Kauffmann, Dr. C. Dolain, Dr. G. Guichard**

United we stand: Oligomers designed to form helix-turn-helix supersecondary structures have been prepared by covalently bridging aliphatic oligourea foldamer helices with either rigid aromatic or more flexible aliphatic spacers. The relative helix orientation in these dimers was investigated by X-ray diffraction and in difficult cases using racemic crystallography. Most X-ray structures reveal well-defined parallel helical hairpin motifs, irrespective of primary sequence and chain length.